Journal of Neuroscience Methods 186 (2010) 42–51

Contents lists available at ScienceDirect

Journal of Neuroscience Methods

journal homepage: www.elsevier.com/locate/jneumeth

Assessing instantaneous synchrony of nonlinear nonstationary oscillators in the brain

Ananda S. Fine [a], David P. Nicholls [b], David J. Mogul [c,*]

[a] University of Illinois, Department of Bioengineering, Medical Scientist Training Program, Chicago, IL, United States
[b] University of Illinois, Department of Mathematics, Statistics and Computer Science, Chicago, IL, United States
[c] Illinois Institute of Technology, Department of Biomedical Engineering, 3255 South Dearborn Street, Wishnick Hall, Room 314, Chicago, IL 60616-3793, United States

ARTICLE INFO

Article history:
Received 27 January 2009
Received in revised form 30 October 2009
Accepted 30 October 2009

Keywords:
Empirical mode decomposition
Hilbert transform
Epilepsy
Nonlinear signal analysis
Eigenvalue decomposition

ABSTRACT

Neuronal populations throughout the brain achieve levels of synchronous electrophysiological activity as a consequence of both normal brain function as well as during pathological states such as in epileptic seizures. Understanding this synchrony and being able to quantitatively assess the dynamics with which neuronal oscillators across the brain couple their activity is a critical component toward decoding such complex behavior. Commonly applied techniques to resolve relationships between oscillators typically make assumptions of linearity and stationarity that are likely not to be valid for complex neural signals. In this study, intracranial electroencephalographic activity was recorded bilaterally in both hippocampi and in anteromedial thalamus of rat under normal conditions and during hypersynchronous seizure activity induced by focal injection of the epileptogenic agent kainic acid. Nonlinear oscillators were first extracted using empirical mode decomposition. The technique of eigenvalue decomposition was used to assess global phase synchrony of the highest energy oscillators. The Hilbert analytical technique was then used to measure instantaneous phase synchrony of these oscillators as they evolved in time. To test the reliability of this method, we first applied it to a system of two coupled Rössler attractors under varying levels of coupling with small frequency mismatch. The application of these analytical techniques to intracranially recorded brain signals provides a means for assessing how complex oscillatory behavior in the brain evolves and changes during both normal activity and as a consequence of diseased states without making restrictive and possibly erroneous assumptions of the linearity and stationarity of the underlying oscillatory activity.

1. Introduction

Synchronous oscillatory activity has been found to be a critical component in both normal brain states such as binding of visual information (Roelfsema et al., 1997; Fries et al., 2001) as well as pathological states such as Parkinson's disease (Levy et al., 2000; Hutchison et al., 2004; Berendse and Stam, 2007), schizophrenia (Gallinat et al., 2004), Alzheimer's disease (Jeong, 2004) and epilepsy (Medvedev, 2002; Le Van Quyen et al., 2003; Dominguez et al., 2005). However, detecting synchronization behavior in the brain represents an extraordinarily difficult problem in neurological science. One of the major issues that arises is determining which features of the signal are to be used in assessing synchrony. For example, synchronization may be simply defined as frequency locking of two signals over some suitably small time window. This frequency locking may be extended beyond 1:1 locking into more complex ratios (e.g. 2:1, 3:2, etc.). A further refinement of frequency locking is phase synchrony detection. Two signals for example may be consistently synchronized with the same or different frequencies but a constant phase shift. In an analysis of this sort, it is first necessary to identify a useful and accurate method for extracting phase from a potentially noisy and multi-component signal and then to examine the phase relationships between two or more of such signals. Although various statistics have been proposed for the detection of phase synchrony from multiple electrodes placed at varying degrees of neuronal resolution (i.e. depth, subdural and/or surface), many of these methods rely on several assumptions that render them inappropriate for detecting synchrony in the brain. All electrophysiological signals besides single cell recordings are a summation of activity from areas surrounding the electrode. In particular, local field potentials (LFPs) represent a sum of dendritic activity that may be inhibitory or excitatory (inhibitory or excitatory post-synaptic potentials, respectively). Thus, waveforms obtained from these areas will be necessarily multi-component.

* Corresponding author. Tel.: +1 312 567 3873; fax: +1 312 567 5707.
E-mail address: mogul@iit.edu (D.J. Mogul).

0165-0270/$ – see front matter © 2009 Elsevier B.V. All rights reserved.
doi:10.1016/j.jneumeth.2009.10.023

All phase synchrony measures rely on prior extraction of phase from the time series, thus one critical step in synchrony analysis is phase determination. Once phase is extracted from a set of signals, the strength of phase coherence between all signals must be measured. A number of statistics have been proposed as a means to measure the strength of phase relationships including mean phase coherence (Mormann et al., 2003), a phase-locking statistic based on wavelet analysis (Lachaux et al., 1999), synchronization time-matrix methods (Lai et al., 2007), enhanced wavelet methods (Roux et al., 2007), and cross-correlation and mutual information measures (Netoff and Schiff, 2002). Many of these methods, while useful, suffer from shortcomings including mixing of amplitude and phase correlations, assumptions on linearity of the underlying signal, and potentially detecting spurious synchrony due to use of a bivariate measure when the signal itself actually represents multiple oscillators with dynamic synchronous behavior. For a non-stationary signal, the most useful method of phase calculation will extract phase values instantaneously. The Hilbert analytic signal method is capable of providing such a measure of phase, but only for mono-component signals. Thus, a prior step to phase calculation will involve some form of filtering of the data.

Most often, filtering of these signals involves either clinically determined ranges (e.g. alpha, beta, etc.) or Fourier spectrum derived bandwidths. Although these bandwidths determined *a priori* may, in many cases, yield useful narrow-band signals, it would be more advantageous for a filtering algorithm to make no assumptions as to the underlying components of the signal under study. Since neurological signals represent nonlinear, nonstationary time series, any analysis method applied to recordings made during normal or pathological brain activity must be capable of retaining these features. Most currently employed methods make assumptions on the phase, frequency and waveform characteristics of the signal without regard to the underlying dynamics of the signal itself.

Besides the ubiquitous Fourier transform method for filtering multi-component signals, other approaches, including wavelet-based and Hilbert transform methods, have been employed to decompose signals to detect phase synchrony. However, as discussed in the next section, many of these methods fail to accurately decompose nonlinear and/or nonstationary signals. Furthermore, almost all of the commonly employed decomposition algorithms assume something about the waveform shape or frequency bandwidth of interest *a priori. A* technique introduced by Huang et al. (1998) termed "empirical mode decomposition" (EMD) filters a multi-component signal into a series of oscillators representing the (adaptively determined) characteristic time-scales of the individual components without *a priori* assumptions of linearity. This method is employed in the current study and discussed further in Section 2.

An ideal analysis method would be capable of extracting proper waveforms adaptively from the time series without the need to build complicated mathematical models derived from first principles (a daunting task for modeling dynamics beyond anything but a small population of neurons). Finally, once the signals have been adaptively filtered, various features of the underlying dynamics must be properly extracted and compared for synchrony. Many methods used for obtaining synchrony information from brain signals do not define the type of underlying oscillators and thus may not be capable of distinguishing the true form of synchrony (if any) present. For example, synchronous behavior can arise as a result of critical detuning between two self-sustained oscillators; alternatively, some neural synchrony may arise as a result of a single self-sustained oscillator driving another system that would not otherwise be capable of oscillatory behavior. Furthermore, many synchrony measures cannot clearly differentiate between frequency and phase synchronized oscillators. For example, two signals may appear to be synchronized due to a measure that detects only frequency locking; this spurious synchrony may actually represent the faithful transmission of an oscillatory signal to another brain area with a phase delay. Thus, the frequency synchrony measured is actually a measure of the same oscillation as it moves spatially. While this is an important dynamic, it does not completely capture the spatiotemporal properties of the signal. Clearly, an ideal synchrony measure would be able to differentiate between these different types of synchrony.

A relatively recent technique combining well-known results in linear algebra and mean-field theory has been proposed to obtain significant synchrony clusters within bivariate phase data measures. In other words, this method proposes to extend simple bivariate measures of phase coherence to a multivariate measure. This method, termed the "eigenvalue decomposition method", utilizes directional statistical features of the phase dynamics between any two oscillatory signals to define significantly synchronized clusters of oscillators (Bialonski and Lehnertz, 2006; Allefeld and Bialonski, 2007). This type of analysis relies on the common assumption that there are several mean fields of globally coupled phase oscillators within the signal set. This approach figures prominently in our new analysis.

We present here an analytic process applied to intracranial EEG information recorded in multiple deep brain nuclei bilaterally in the rat that merges the techniques of empirical mode decomposition, Hilbert analytic signal method, mean phase coherence measures and finally eigenvalue decomposition to ultimately identify complex instantaneous synchronous behavior. This method allows for the possibility of multiple underlying oscillators and can potentially detect dynamic changes in phase synchrony that may be spatiotemporally nonstationary. Such a procedure may provide important new insights as a seizure or any other complex neurological process in the brain evolves in time and space.

2. Materials and methods

2.1. Surgical procedure and data acquisition

Male Sprague-Dawley rats, 48–57 days old and weighing approximately 225–280 g were used in this study. Experiments were conducted in accordance with the National Institutes of Health for the care and use of laboratory animals. Rats were anesthetized by a mixture of ketamine (70 mg/kg) and xylazine (2 mg/kg) delivered intraperitoneally. All procedures were performed in a Kopf stereotactic frame (KOPF Model 900, CA, USA). Stereotactic targets were calculated using a stereotactic rat brain atlas (Paxinos and Watson, 2006). Lambda, bregma and sagittal sutures were used as landmarks to navigate to the desired stereotactic points. The skull was perforated using a high speed stereotactic drill (Micromotor™ Drill, Stoelting Co, IL USA) with 1.2–2 mm diameter drill tips. Bipolar electrodes surrounding a single stainless steel injection cannula in one integrated electrode assembly (C315G-MS 303: PlasticsOne, Roanoke, VA, USA) were stereotactically implanted into the CA3 region of the left hippocampus (−3.5 mm bregma, 2.8 mm lateral, 3.7 mm deep). Bipolar recording electrodes (without cannula) were implanted into the contralateral hippocampus and anteromedial thalamus (−1.8 mm bregma, 0.3 mm lateral, 6.1 mm deep). After injection of epileptogenic chemicals into the CA3 region of the left hippocampus, the internal cannula insert was withdrawn and a 100 μm diameter stainless steel insert was threaded through the cannula to provide one side of the recording pair. The reference electrode used was the skull stabilization screw most proximal to the electrode assembly. After conclusion of the experiment, histological verification of electrode placement and tissue damage was assessed via formalin fixation and subsequent Nissl staining. We used a chemical induction model of epilepsy in order to induce a physiological state that

has been classically described as "hypersynchronous". Each experiment involved recording one half hour of baseline activity followed by focal injection of 3–5 nmol kainic acid into the CA3 region of the left hippocampus.

2.2. Empirical mode decomposition

Traditional spectral decompositions applied to time series usually involve an assumption that the underlying signal dynamics consist of a linear superposition of complex exponentials. However, these radial basis functions are always assumed *a priori* rather than obtained adaptively from the signal. If the signal of interest contains more than just pure low frequency sine and cosine functions, the resulting power spectrum obtained from Fourier analysis, for example, will contain spurious power readings and energy spreading that actually represent nonlinearities in the data. This is because nonlinearities in the data will be represented within the Fourier power spectrum as higher-order harmonics since the transform itself utilizes a superposition of trigonometric functions. However, once the transform has been implemented, it is difficult to distinguish true power-frequency readings from spurious energy spreading due to nonlinearities inherent within the system. Furthermore, Fourier transform methods require piecewise stationarity of the time series under study. Thus any time-varying frequency content (usually present within EEG data) will be averaged out in the power spectrum. Although calculation of Fourier spectrograms, involving computation of the Fourier power spectrum over short time windows and plotting these power readings over time, has been proposed as a means to detect nonstationarity, this method still relies on linearity of the time series. Ideally, a decomposition method would be capable of extracting underlying oscillators from a seizure signal without any assumptions of the underlying waveform or characteristic time-scales of the oscillators. Recently, Huang et al. (1998) introduced EMD, a method for the extraction of (potentially nonlinear and nonstationary) oscillators from any time series in an adaptive fashion.

The EMD can be characterized as an adaptive, data driven decomposition that results in a series of intrinsic mode functions (IMFs) that together comprise the underlying oscillations (or basis functions) within a dataset. The basis functions are determined from the dynamics of the signal itself. Any time series may be represented as a linear combination of oscillators:

$$x(t) = \sum_{j=1}^{N} a_j \phi_j(t). \quad (1)$$

In Fourier decomposition, for example, each $\phi_j(t)$ is a sine or cosine with a corresponding Fourier coefficient, a_j, for each $\phi_j(t)$. In order to improve the decomposition of a time series to account for nonstationarity, other decompositions such as wavelet analysis have been applied; however, while they allow for nonstationarity, the basis functions are, again, determined before the decomposition and thus may be inappropriate for nonlinear signals. The properties of nonlinearity and nonstationarity are very likely intrinsic to neurological signaling rather than merely artifacts of noise, instrumentation or other experimentally imposed conditions, thus it is vital to capture these properties in the applied analysis.

The EMD has been mainly applied to hydrologic (Sinclair and Pegram, 2005), atmospheric (Salisbury and Wimbush, 2002), oceanic (Schlurmann, 2002) and geologic (Zhang et al., 2003) time series, but it is widely believed to be applicable to any time series. The method can be briefly outlined as follows: The decomposition begins by identifying all maxima and minima of the dataset followed by interpolation between the extrema using a cubic spline to obtain a maximum envelope $e_{\max}(t)$ and a minimum envelope $e_{\min}(t)$. Next, the average of the envelopes $m(t) = [e_{\max}(t) + e_{\min}(t)]/2$ is computed and subtracted from the original data $x(t)$ to obtain a residual $r(t) = x(t) - m(t)$. This process is then repeated on the residual in an iterative fashion to obtain a series of IMFs. Because this is a numerical approximation scheme, the procedure must be refined by sifting the data through iteration of the first few steps (prior to subtraction of the mean) to obtain a zero-mean amplitude- and frequency-modulated signal which may be called a "proper rotation" or an IMF. Practically, the sifting process is optimized according to the particular dataset by defining an appropriate stopping criterion using, for example, number of sifts (Huang et al., 1998), accumulated energy (Chen and Feng, 2003), or confidence limit criteria (Huang et al., 2003). After the sifting and iteration procedure is complete, one obtains a series of modes plus the "trend" that represents the remainder of the decomposition when further sifting will not result in a proper IMF.

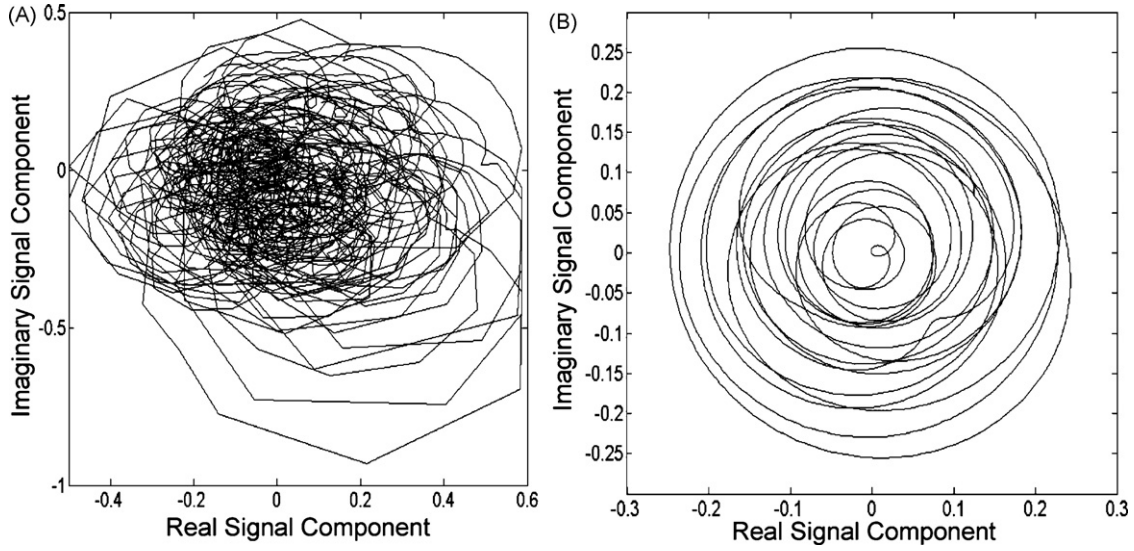

Fig. 1. Hilbert analytic signal. (A) Three seconds of an unfiltered seizure signal demonstrates the ambiguous nature of phase determination from the analytic signal. (B) Three seconds of the corresponding signal after filtering via EMD. Due to the nature of the construction of IMFs, phase can be clearly measured from the analytic signal. Axes represent the real (abscissa) versus the imaginary (ordinate) component of the analytic signal.

2.3. Analytic signal method

There are a number of methods available for calculating phase but the most appropriate to use for instantaneous phase measurements from narrowband signals is the Hilbert analytic signal method (Gabor, 1946). This method is only appropriate in the case of a narrowband signal because multi-component signals will yield a trajectory in the complex plane that has multiple centers of rotation. For an unambiguous determination of phase, the complex trajectory of the analytic signal must have only a single center of rotation, thus this method requires prior filtering of the signal. As we shall see, the IMFs produced by the EMD have precisely this property.

In an EMD, if each IMF is taken as its own time series, one then obtains a group of analytic signals whose amplitude and phase are defined instantaneously via the following relation:

$$s_j(t) = x_j(t) + iH_j(x_j(t)) = A_j(t)e_j^{i\phi(t)} \quad (2)$$

with

$$A_j(t) = (x_j(t)^2 + H_j(x_j(t))^2)^{1/2} \text{ and } \phi_j(t) = \tan^{-1}\left[\frac{(Im(s_j(t))}{Re(s_j(t))}\right], \quad (3)$$

where $H_j(t)$ is the Hilbert transform of the jth IMF. This technique is a well-known method to obtain the analytic representation of a time series. According to the Cauchy–Riemann equations, if the real component of a signal is known, the corresponding imaginary component may be obtained via the Hilbert transform. This can then be equated via Euler identities to a value determining the analytic phase $\phi(t)$ and amplitude $A(t)$, as shown in Eq. (3). In general, the Hilbert transform is a convolution that will shift the signal's phase by $\pi/2$:

$$H[x(t)] = pv\int_{-\infty}^{\infty} x(\tau)h(t-\tau)\mathrm{d}\tau), \quad (4)$$

where pv indicates that the integral should be taken as the Cauchy principal value because the function $h(t) = 1/\pi t$ is not integrable and thus the convolution integral will not converge. One of the major limitations of merely performing a Hilbert transform for determination of instantaneous phase and frequency is that the bandwidth of interest must be defined *a priori*. This means that one must not only artificially restrict the analysis but, more importantly, if the signal contains a multi-component or time-varying spectrum, the resulting signal will contain multiple centers of rotation in the phase space reconstruction. Each rotation center represents another oscillator; for example, a sine wave reconstruction in the complex plane will have a single center, represented as an isolated circle. Any signal with multiple underlying oscillator components will have multiple centers of rotation. Furthermore, if the signal is nonstationary, this will be reflected in the complex plane as multiple windings around each component center. This suggests that the instantaneous phase determined in this way may vary, depending on which of the dominant rotations we choose. Although trial-and-error could yield useful results on which of the various rotations represents the proper phase to use for further analysis, it would be more useful to be capable of directly extracting and visualizing the underlying frequency components contributing to the multiple centers of rotation. The EMD process described above allows for determination of a proper phase by isolating underlying basis functions (IMFs) that yield phase space rotations with only one center and an unambiguous phase measure. Fig. 1 demonstrates the trajectory of a signal submitted to Hilbert transform without prior filtering and for an IMF obtained from empirical mode decomposition, depicting the necessity for prior filtering for proper usage of the Hilbert transform in obtaining an analytic signal with an unambiguous phase.

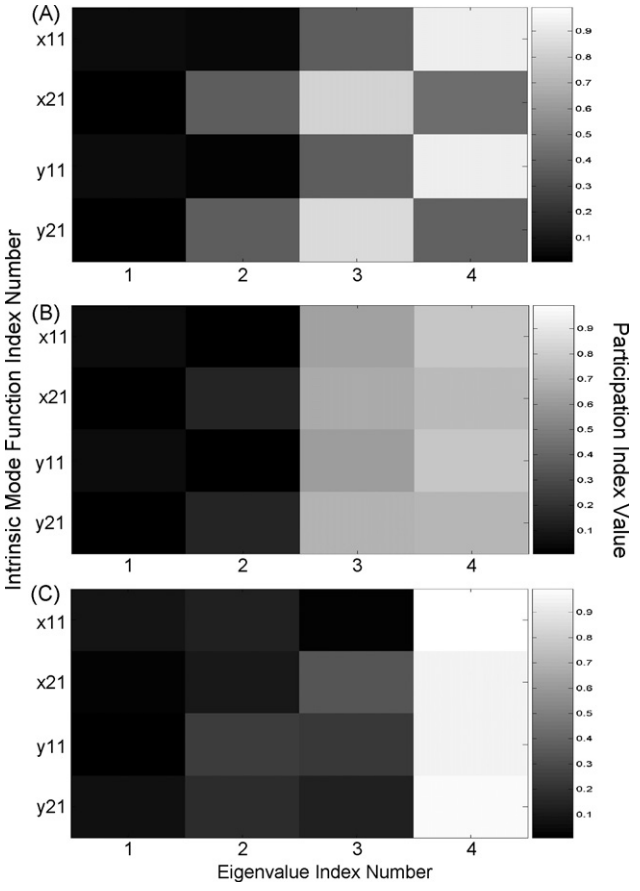

Fig. 2. Clustering in two coupled Rössler attractors validates eigenvalue decomposition. (A) Uncoupled, (B) moderate coupling and (C) fully coupled.

2.4. Eigenvalue decomposition method

Once the highest energy IMFs are obtained from each channel within a data segment, it is desirable to determine the strength of synchrony between oscillators. To accomplish this, each IMF is treated as a row vector and compiled into an m x n matrix, where m is the number of IMFs obtained from the analysis and n is the length of the time series. This set of time series represents the significant oscillators decomposed from the original time series via EMD. Next, the mutual phase coherence is calculated (Mormann et al., 2003); this quantity is defined as

$$R_{mn} = \sum_{\substack{k=1 \\ m \neq n}}^{N} \exp[i(\phi_{nk}(t) - \phi_{mk}(t))], \quad (5)$$

where "exp" represents the exponential, "i" is $\sqrt{-1}$, and each $\phi(t)$ is the phase of the analytic signal pair (indicated by subscripts m and n) sampled at each discrete time instant from $k = 1$ to N (the number of time points in the series). The mean phase coherence values are normalized and range from 0 to 1 with maximum mean phase coherence obtained at 1. Because this matrix thus obtained is square symmetric, one can perform an eigenvalue decomposition to project the mean phase coherence values for the entire set of oscillators onto a set of vectors representing the preferred direction of the mean phase field. These preferred directions are the principal eigenvectors. For any eigenvalue–eigenvector pair, a phase correlation value may be assigned as the strength of the connection of

a given eigenvalue and the coefficient of each IMF within the associated eigenvector. Furthermore, each eigenvalue is ordered, with the largest eigenvalue representing the most strongly correlated cluster with the participation of each oscillator in a given cluster quantified by the value of the eigenvector. Specifically, one can assign the strength of the connection (participation) between the phases of any two IMFs within a single group via the square root of each eigenvalue (λ_n) multiplied by the component-wise square of the associated eigenvector (v_1^2):

$$\sqrt{[\lambda_1 v_1^2]} \tag{6}$$

For example, if a matrix of completely unsynchronized oscillators is analyzed in this way, one would obtain $\lambda_1 = \lambda_2 = \ldots = \lambda_1 = 1$ with $v_1 = (0, \ldots, 0, 1, 0, \ldots, 0)$and no clusters would be identified in Eq. (6). If a set of fully synchronized oscillators is analyzed, one would obtain a single eigenvalue, whose value is identical to the number of oscillators with $v_1 = (1, \ldots, 1)$ and a single cluster in Eq. (6). Finally, for a set of oscillators with varying levels of synchrony, one would obtain a set of (strictly positive) eigenvalues. Those eigenvalues above one are considered significant and the components of their eigenvectors identify participation in the corresponding cluster calculated via Eq. (6). This threshold is set because, if a set of uncorrelated eigenvalues becomes more correlated, any increase in the eigenvalue must be offset by a corresponding decrease in other eigenvalues (as the sum of the eigenvalues is conserved). The eigenvalue decomposition method as cluster analysis is introduced and described in detail in Allefeld and Bialonski (2007).

3. Results

3.1. Synchronized Rössler model

To test the reliability of the algorithm described in this thesis, we constructed a set of time series drawn from two coupled Rössler oscillators. These chaotic oscillators were studied by Rosenblum et al. (1996) and shown to have characteristic phase synchronization properties at specific parameters. The model itself is represented by two nearly identical Rössler oscillators coupled via a parameter C with frequencies ω_1 and ω_2. Both the coupling constant and

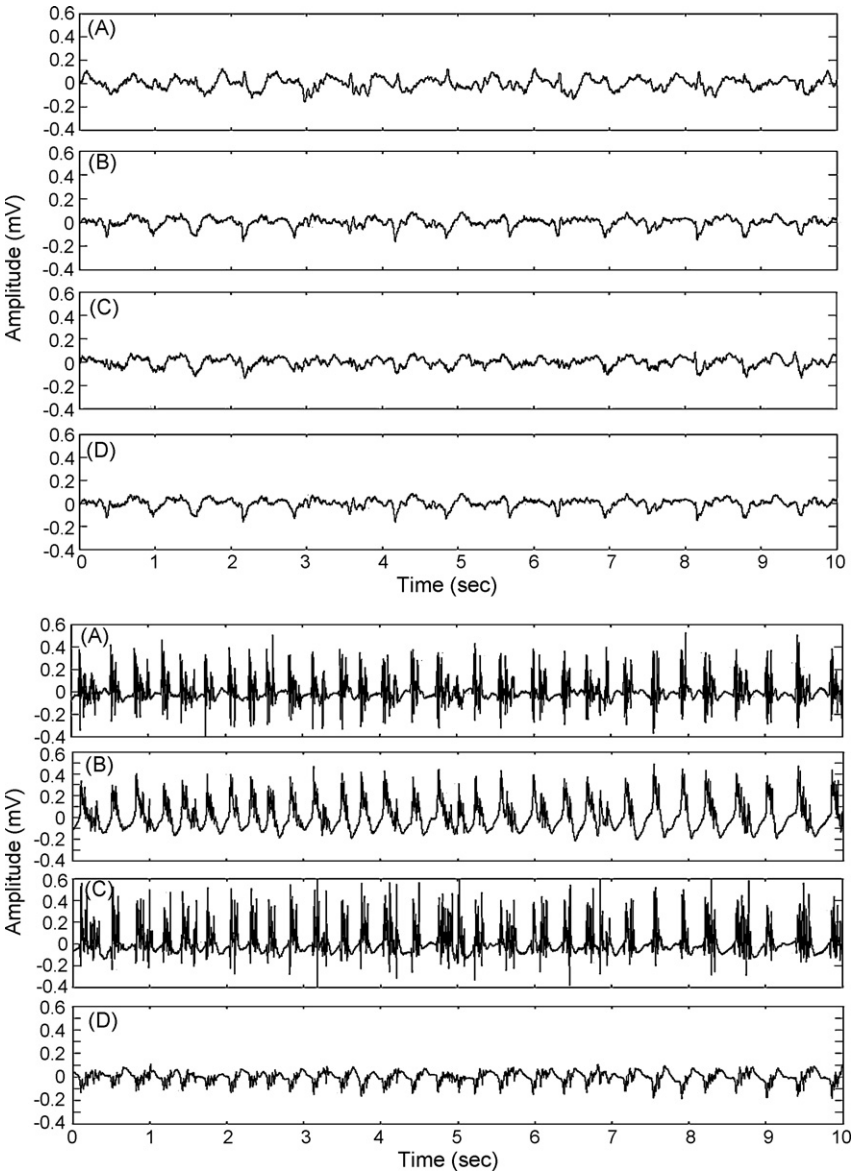

Fig. 3. 10 second samples of recorded LFP data. (Top) Prior to kainic acid exposure and (bottom) after kainic acid exposure. (A) Focal hippocampus. (B) Anteromedial thalamus. (C) Contralateral hippocampus. (D) Subdural recording over contralateral hemisphere.

frequency mismatch will affect the level of synchronization.

$$\begin{aligned}\frac{dx}{dt} &= -\omega_{1,2}y_{1,2} - z_{1,2} + C(x_{2,1} - x_{1,2})\\ \frac{dy}{dt} &= \omega_{1,2}x_{1,2} + 0.15y_{1,2}\\ \frac{dz}{dt} &= 0.2 + z_{1,2}(x_{1,2} - 10)\end{aligned} \tag{7}$$

As described in the abovementioned paper, by keeping the frequency mismatch constant we can vary the coupling parameter to achieve a state of synchronous ($C = 0.035$), nonsynchronous ($C = 0.01$) and nearly synchronous ($C = 0.027$) oscillation between the two systems. For our simulation, we used $\omega_1 = 1.5$ and $\omega_2 = 2.0$. For simplicity, we used the output of x_1, x_2, y_1, and y_2 as the input time series for the analysis. This is an advantageous combination because the x_1–y_1 and x_2–y_2 pairs are expected to be synchronized regardless (because they are drawn from the same system) while the combinations coming from the two different systems (x_1–x_2 and y_1–x_2) will be expected to have varying synchronization levels depending on the value of C. Fig. 2 shows the eigenvalue decomposition matrix obtained for the nonsynchronized (A), almost synchronized (B) and fully synchronized (C) regimes. This matrix serves as the output of the entire algorithm described previously. That is, each time series (x_1, x_2, y_1, y_2) was submitted to empirical mode decomposition and the intrinsic mode functions were processed through the eigenvalue decomposition and assigned a participation value according to the preferred direction of phase within each eigenvector. In part A the oscillators being to separate themselves into distinct clusters with no interaction between the two systems; i.e. with the x_1–y_1 pair participating in one cluster (with the same frequency) and the x_2–y_2 pair participating in another cluster. In part B the participation values for each of the obtained oscillators is diffuse with no clear synchrony for any oscillator as the coupling parameter attempts to bring all frequencies closer together. In part C, the oscillators are fully synchronized (despite an initial frequency mismatch) and all participate in one cluster.

3.2. Experimental data analysis

Depth recordings of brain activity were made from the CA3 region of the hippocampus bilaterally as well as in the anteromedial thalamus (targeted stereotactically) and over the surface of one hemisphere (contralateral to the hippocampus focally injected with kainic acid) in four rats. Both baseline and induced seizure activity were recorded for subsequent analysis. Fig. 3 shows a 10-s sample prior to kainic acid (KA) exposure (top) and after KA exposure (bottom). As can be readily seen, electrical activity recorded after KA exposure is higher in frequency and amplitude than pre-exposure activity. Furthermore, this activity can be seen at all four electrode sites. Visual inspection suggests a high degree of synchrony between all four electrode sites. Furthermore, the signals originating in both hippocampi appear more similar in waveform

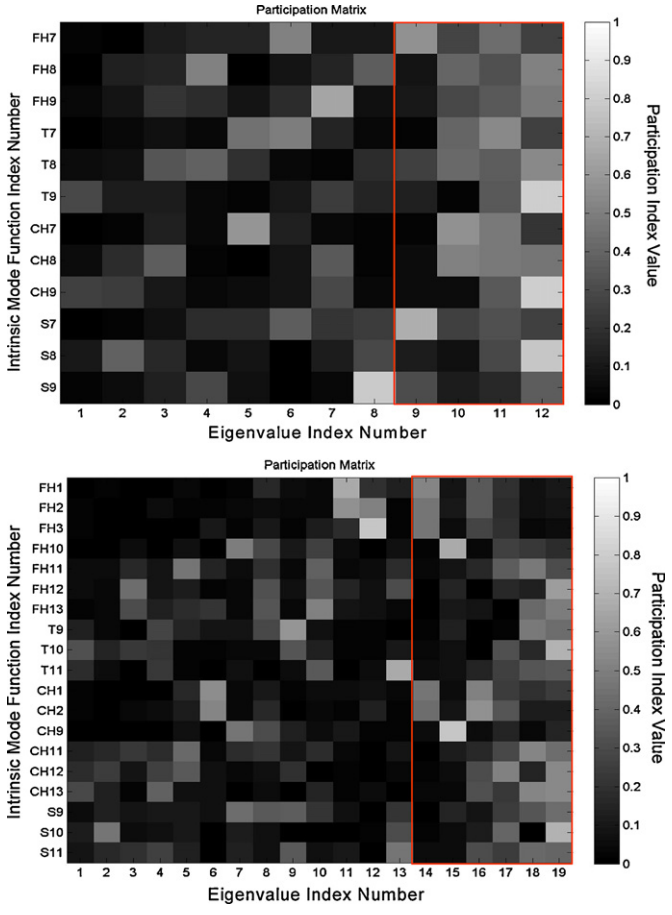

Fig. 4. Participation matrix. (A) Pre-exposure and (B) post-exposure. Abscissa shows the eigenvalue index number (not the eigenvalue itself) with $\lambda_1 < \lambda_2 < \ldots < \lambda_n$. Ordinate shows intrinsic mode function index; FH: focal hippocampus, T: anteromedial thalamus, CH: contralateral hippocampus, S: subdural electrode over the hemisphere contralateral to seizure induction. Gradient scale indicates participation strength. Red box demarcates significant clusters (whose eigenvalues are greater than one). (For interpretation of the references to color in this figure legend, the reader is referred to the web version of the article.)

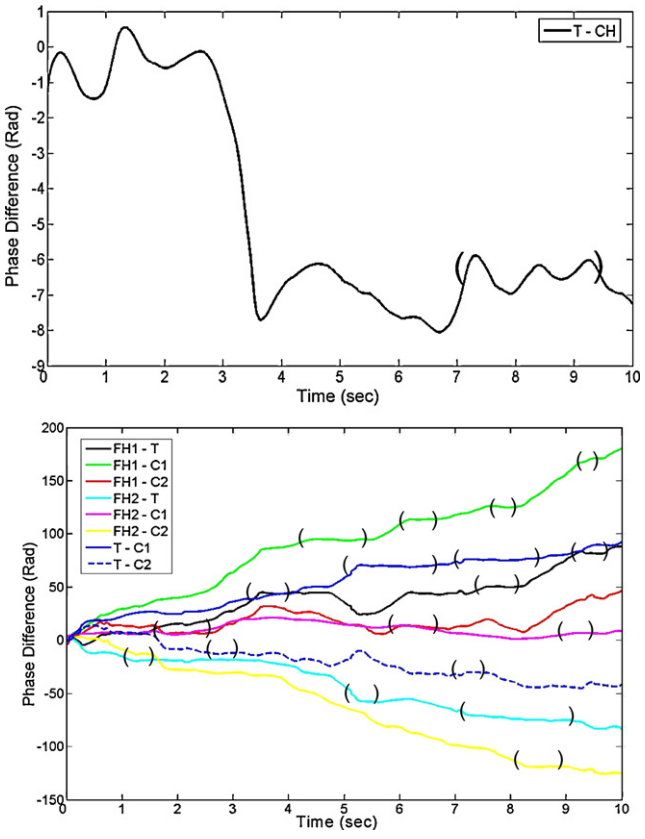

Fig. 5. Largest participation cluster phase differences. (A) Pre-exposure: the largest eigenvalue participation cluster in the interictal sample contained two thalamus (T) IMFs and one contralateral hippocampus (CH) IMF. (B) Post-exposure: the largest eigenvalue participation cluster in the ictal sample contained two focal hippocampus (FH) IMFs, one thalamus (T) IMF, and two contralateral hippocampus (CH) IMFs. Areas where the phase difference is constant (indicated by parentheses) represent synchronous epochs.

to one another than to anteromedial thalamus or the subdural signal. It should be noted that all recordings represent brain activity in an anesthetized rat, as these are all acute *in vivo* studies. Thus, recordings made in these anesthetized animals show some level of pre-seizure synchrony most likely due to the activity of the anesthetic on the brain.

Seizures are generally thought to represent aberrantly synchronized neural activity. Therefore, we sought to develop an algorithm to accurately assess and quantify this synchrony. The most relevant features of an oscillating signal to use for synchrony analysis are the phase or frequency. However, the raw signal must be filtered in some way prior to measuring these quantities. The EMD accomplishes this task without any assumptions as to the underlying waveforms. Once the signals have been decomposed in this way, the highest energy oscillators were selected for further synchrony analysis. A low threshold for IMF exclusion was utilized to determine selected oscillators (in order to eliminate as few as possible) by calculating the mean squared energy (MSE) amplitude and ignoring those intrinsic mode functions whose MSE fell below one standard deviation above the mean energy. In general, this cutoff eliminated intrinsic mode functions that consisted primarily of instrumentation noise.

The Hilbert analytic signal was constructed for each IMF in order to calculate the instantaneous phase for all selected IMFs. Then, the mean phase coherence was calculated for the entire matrix of phase values from each 10-s sample. Finally, the eigenvalue decomposition was performed on this new mean phase coherence matrix to identify significantly synchronized clusters. A summary of all values of the participation index for these samples is shown in Fig. 4: (A) pre-exposure and (B) post-exposure samples corresponding to

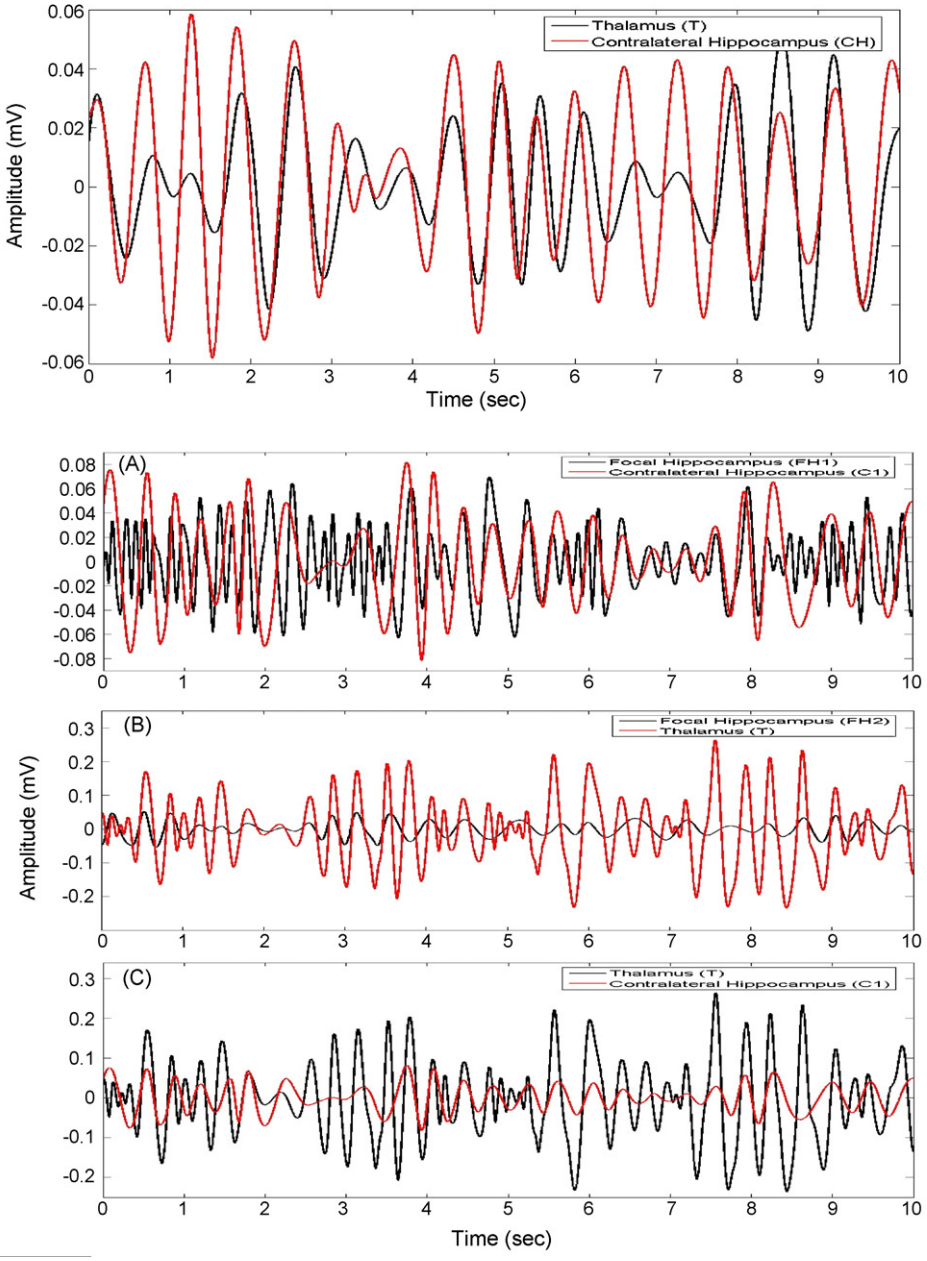

Fig. 6. Selected IMF comparisons from most significant cluster, seizure. (Top) Pre-exposure, thalamus IMF (1) superimposed on contralateral hippocampus IMF. (Bottom) Post-exposure, (A) Focal hippocampus (1) IMF superimposed on contralateral hippocampus IMF. (B) Focal hippocampus (2) IMF superimposed on thalamus IMF. (C) Thalamus IMF superimposed on contralateral hippocampus IMF. All IMFs are taken from the most significant cluster. Note phase synchronized regions (corresponding to areas demarcated by parentheses in Fig. 4) do not necessarily have amplitude matching.

those in Fig. 2. The red box indicates those clusters which are identified as significant (eigenvalues greater than 1). In general, interictal and baseline cluster analyses reveal overall fewer clusters than the same analysis for seizure samples. For the representative analysis samples shown in Fig. 3, the pre-exposure sample revealed four significant clusters while the post-exposure sample showed six.

In order to highlight the instantaneous synchronous relationship between oscillators participating in a given cluster, the difference between the phases for each oscillator pair in the most significant cluster (highest eigenvalue) was calculated and plotted in Fig. 5. These plots demonstrate the phase dynamics of the entire cluster. Because these oscillators are noisy, there are a number of phase slips (i.e. a change in the phase difference of 2π). However, those areas where the phase difference remains approximately constant represent regions of synchronization. These regions of approximately constant phase were defined when the ratio of the two phases was between 1 and 1.3 (i.e. when the slope of the phase difference was approximately constant). Several of these areas of phase synchronization are highlighted in the figure by parentheses. Oscillators originating from the subdural electrode were not included in this analysis because these signals represent a summation of all activity within the (large) hemispheric dipole. Therefore, much of the activity recorded on that channel is contained within recordings made from subcortical sites. Thus, any synchrony between these oscillators and those obtained from depth sites is likely to be spurious because there will be high

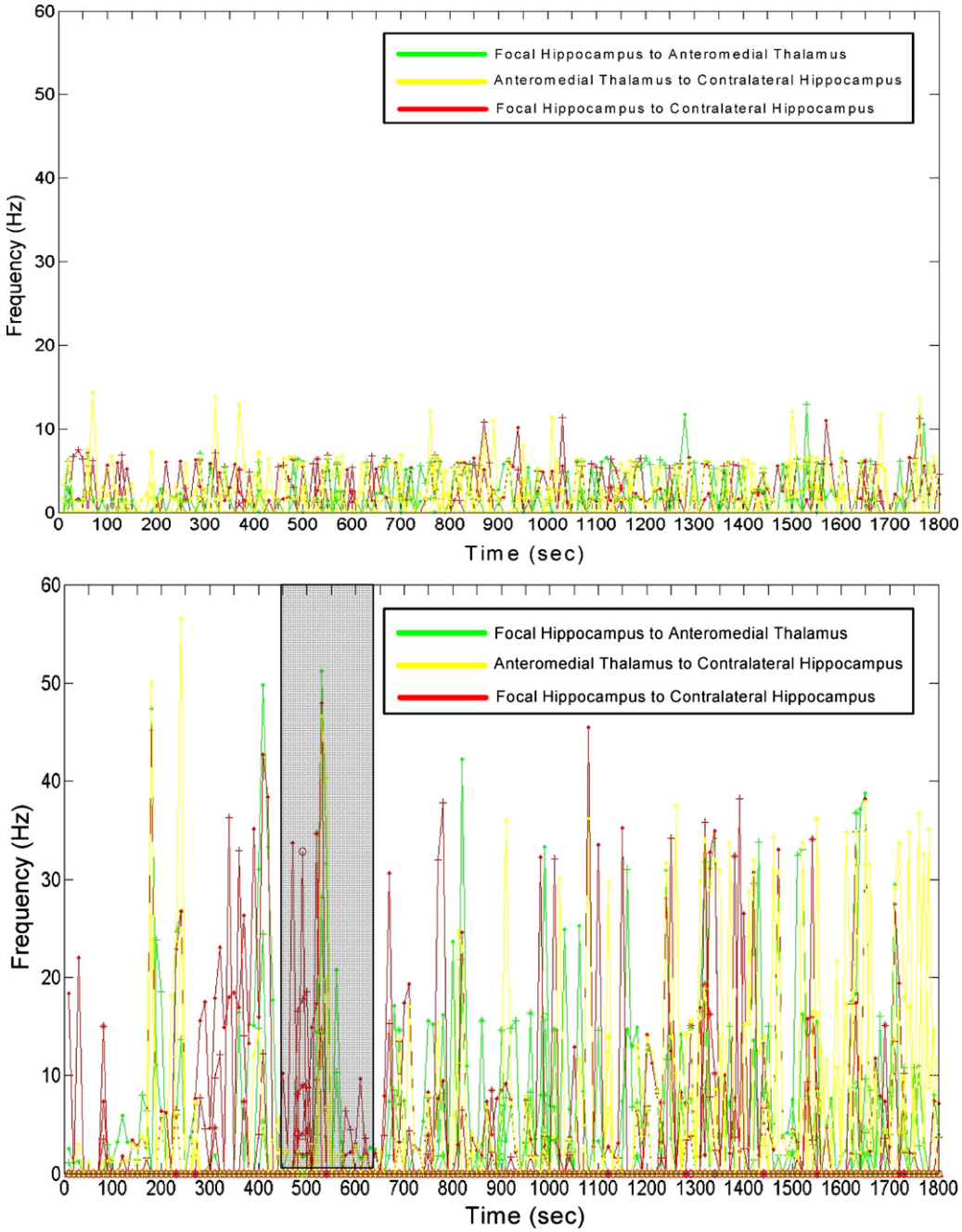

Fig. 7. Frequency of synchrony summary. (Top) Pre-exposure to KA. (Bottom) Post-exposure. Episodes of phase locking between each nucleus are indicated with the average frequency between the two oscillators. (*Green*): Focal hippocampus to anteromedial thalamus synchrony, (*yellow*): anteromedial thalamus to contralateral hippocampus synchrony, (*red*): focal hippocampus to contralateral hippocampus synchrony. All significant clusters forming mean fields are summarized. Shaded box represents region highlighted in Fig. 8. (For interpretation of the references to color in this figure legend, the reader is referred to the web version of the article.)

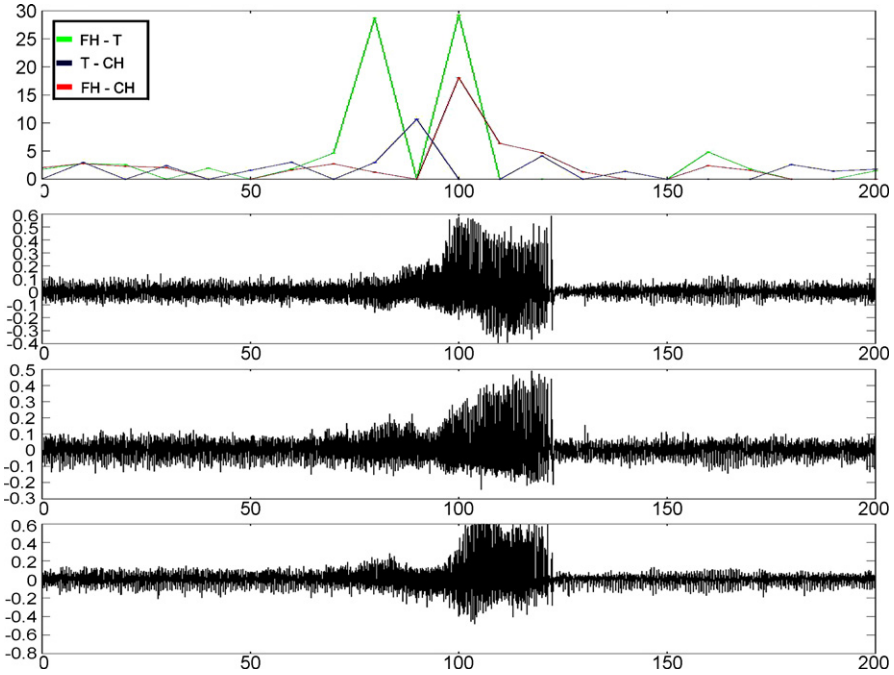

Fig. 8. Frequency of synchrony for representative seizure. (Top) Frequencies of synchronization are shown for the *top cluster* only of the time region indicated by the shaded box in Fig. 7 (in 10 s bins). (*Green*): Focal hippocampus to anteromedial thalamus synchrony, (*blue*): anteromedial thalamus to contralateral hippocampus synchrony, (*red*): focal hippocampus to contralateral hippocampus synchrony. (Bottom) Local field potentials for the three recorded nuclei. (For interpretation of the references to color in this figure legend, the reader is referred to the web version of the article.)

synchrony between identical oscillators. The post-exposure sample shows not only more oscillators, but also more regions of phase synchrony than the pre-exposure samples. Furthermore, the phase synchrony is not constant between any two brain areas. Instead, the synchrony changes between different brain nuclei over time. Fig. 6 further illustrates these synchronous epochs by superimposing two participating oscillators in a given cluster. Clearly, those times where the oscillators overlap in phase (not necessarily in amplitude) represent synchronous epochs. To summarize the frequencies of instantaneous phase synchrony, periods of time at which the frequencies of two oscillators were locked during a full half hour of recording is plotted in Fig. 7. These plots demonstrate a combined average frequency between two oscillators during episodes of frequency locking. Each nucleus pair (focal hippocampus, anteromedial thalamus or contralateral hippocampus) is represented by a different color, with green indicating frequency locking episodes between the focal hippocampus and anteromedial thalamus, yellow indicating anteromedial thalamus and contralateral hippocampus frequency locking and frequency locking between the two hippocampi indicated in red. It must be noted that the frequencies represent a combined average between two oscillators during significantly synchronized episodes as obtained by the eigenvalue decomposition. By comparing the pre-exposure to post-exposure plots, it is evident that the pre-exposure frequencies are lower and that the distribution of frequency locking episodes among the nuclei is more uniform. The post-exposure frequencies are higher and also show more variability. Furthermore, the density of synchronous episodes is much higher during seizure episodes. To further illustrate these synchronization events, a representative seizure and the corresponding synchronization frequencies are shown in Fig. 8. Only the top cluster of synchronization is shown in this plot for clarity. It is evident from this plot that there is an increase in focal hippocampus to anteromedial thalamus synchrony as the seizure begins, followed by an increase in anteromedial thalamus to contralateral hippocampus synchrony as the seizure evolves and finally, an increase in focal hippocampus to contralateral hippocampus synchrony as the seizure ended. This general pattern of change in synchronization among nuclei was generally (though not always) observed consistently within this animal. However, different animals displayed unique synchronization patterns reflecting variability in seizure dynamics across animals similar to that seen in human seizures.

4. Discussion

Synchronized activity is implicated at all levels of neural activity in both pathological and normal states. It may be that both long- and short-range synchronization throughout the brain is a normal component of sensory and cognitive processing and that pathological states represent a derangement of this normal synchronization behavior. However, in order to characterize this synchrony in either pathological or normal states, it is necessary first to define a measure that is capable of detecting any form of synchrony that may arise. It is suggested here that prior filtering of a time series by a means that presupposes the underlying waveform and/or frequency content of the signal may eliminate important features of the signals underlying phase synchrony dynamics. Therefore, it is proposed that a dynamic filter such as empirical mode decomposition is first employed in order to isolate any underlying oscillators. However, one important consideration in utilizing this technique is whether these intrinsic mode functions represent actual physiological oscillators or merely depict the phase dynamics of one or more physiological oscillators. This limitation is unlikely to interfere with synchrony analysis, but it may cause problems with direct physical interpretation of the oscillators obtained from the decomposition. Nevertheless, no other decomposition method to our knowledge is capable of yielding true physical oscillators at this point as all of them rely on some assumption as to the oscillator waveforms underlying the signal and usually involve fitting the time series to some *a priori* determined wave (e.g. a sine wave).

Since Penfield and Jasper reported in 1954 that pathologically synchronized activity may underlie seizures, numerous experiments have been performed to attempt to identify this activity in seizure networks. However, it is, as yet, unclear if seizures can be simply described as a highly synchronized state or if there are more complex synchronized and desynchronized neural dynamics underlying the generation, maintenance and propagation of seizure activity. It has been suggested that a seizure represents a 'resetting' of neural signaling that has degenerated to a disordered state of wrongly synchronized and desynchronized local neural networks. Using mean phase coherence as a measure of phase synchrony, Mormann et al. (2003) recently reported that there is a state of decreased synchronization just prior to an epileptic seizure that is marked by a high degree of variability in synchronization followed by a return to baseline (relatively high) levels of synchronization. This variability, however, might represent an increase in the number of oscillators, each of which participates in a synchronous relationship with one or more of the other oscillators. As our study suggests, seizures tend to contain many more oscillators than the pre-ictal or interictal state. Furthermore, the synchronicity between these oscillators is not constant. Instead, the synchrony seems to shift between the oscillators within and between subcortical nuclei participating in the seizure circuit. A measure such as mean phase coherence alone is unable to distinguish this fine spatiotemporal synchrony and thus merely shows high variability in the synchrony value.

In a study utilizing and comparing various measures of phase synchrony, including mutual information, cross-correlation and phase correlation, Netoff and Schiff (2002) also observed a decrease in phase synchrony just prior to chemically induced epileptogenic events in the CA1 region of hippocampus slice preparations. However, many of these measures mix amplitude and phase correlations. Amplitude correlation might suggest more neurons participating in the synchronous oscillator, while phase correlations suggest that neurons already participating in the oscillations are becoming more synchronized. Both types of correlations are important, but they represent different results and thus must be distinguished from one another. A decrease in synchrony as measured by a computation that mixes amplitude and phase might represent a decrease in the absolute number of neurons participating or an actual decrease in the synchrony, or both. This suggests that there may be a more complex fine structure underlying the seizure dynamics that may be explored via phase analysis. However, the phase synchronization measurements used in earlier studies did not always give the same significance level for phase synchronization; furthermore, applying the measurements to broad-band and narrow-band filtered time series data gave different results. Thus, these results highlight the importance of the chosen algorithm for extracting frequency, phase and phase synchrony measures for accurate determination of phase information.

There is a general consensus that seizure dynamics represent some form of pathological synchrony in various brain areas. However, there is no general agreement on how this synchrony arises (e.g. by decreased inhibitory feedback or increased excitatory input) or even how to measure and detect this proposed synchronous behavior. Synchrony in seizure dynamics may arise as a result of two or more self-sustained oscillators interacting to produce a pathological synchronous state. This possibility requires that the individual oscillators' frequency detuning (mismatch) is sufficiently small such that the oscillators' phase dynamics may align. Alternatively, the proposed synchronous state may arise as a result of stochastic resonance between two or more oscillators. A final alternative explanation may be that one or more oscillators arise within a pathological neural network that then serve as a driving force for anatomically or functionally connected networks, giving rise to seizure propagation. Any or all of these types of synchronous behavior may be responsible for seizure dynamics.

Acknowledgement

We would like to thank Dr. Yue Li for his excellent assistance in developing the software for on-line recording and analysis of seizure signals in the rat.

References

Allefeld C, Bialonski S. Detecting synchronization clusters in multivariate time series via coarse-graining of Markov chains. Phys Rev E Stat Nonlin Soft Matter Phys 2007;76(6 Pt 2):066207.
Berendse HW, Stam CJ. Stage-dependent patterns of disturbed neural synchrony in Parkinson's disease. Parkinsonism Relat Disord 2007;13(Suppl. 3):S440–5.
Bialonski S, Lehnertz K. Identifying phase synchronization clusters in spatially extended dynamical systems. Phys Rev E Stat Nonlin Soft Matter Phys 2006;74(5 Pt 1):051909.
Chen Y, Feng MQ. A technique to improve the empirical mode decomposition in the Hilbert–Huang transform. Earthquake Eng Eng Vib 2003;2(1):75–85.
Dominguez LG, Wennberg RA, Gaetz W, Cheyne D, Snead OC, Velazquez JLP. Enhanced synchrony in epileptiform activity? Local versus distant phase synchronization in generalized seizures. J Neurosci 2005;25(35):8077–84.
Fries P, Reynolds JH, Rorie AE, Desimone R. Modulation of oscillatory neuronal synchronization by selective visual attention. Science 2001;291(5508):1560–3.
Gabor D. Theory of communication. J IEEE Lond 1946;93(26):429–57.
Gallinat J, Winterer G, Herrmann CS, Senkowski D. Reduced oscillatory gamma-band responses in unmedicated schizophrenic patients indicate impaired frontal network processing. Clin Neurophysiol 2004;115(8):1863–74.
Huang NE, Shen Z, Long SR, Wu MC, Shih HH, Zheng Q, et al. The empirical mode decomposition and the Hilbert spectrum for nonlinear and non-stationary time series analysis. Proc R Soc Lond A 1998;454:903–95.
Huang NE, Wu M-LC, Long SR, Shen SSP, Qu W, Gloersen P, et al. Confidence limit for the empirical mode decomposition and Hilbert spectral analysis. Proc R Soc Lond A 2003;459:2317–45.
Hutchison WD, Dostrovsky JO, Walters JR, Courtemanche R, Boraud T, Goldberg J, et al. Neuronal oscillations in the basal ganglia and movement disorders: evidence from whole animal and human recordings. J Neurosci 2004;24(42):9240–3.
Jeong J. EEG dynamics in patients with Alzheimer's disease. Clin Neurophysiol 2004;115(7):1490–505.
Lachaux JP, Rodriguez E, Martinerie J, Varela FJ. Measuring phase synchrony in brain signals. Hum Brain Mapp 1999;8(4):194–208.
Lai YC, Frei MG, Osorio I, Huang L. Characterization of synchrony with applications to epileptic brain signals. Phys Rev Lett 2007;98(10):108102.
Le Van Quyen M, Navarro V, Martinerie J, Baulac M, Varela FJ. Toward a neurodynamical understanding of ictogenesis. Epilepsia 2003;44(Suppl. 12):30–43.
Levy R, Hutchison WD, Lozano AM, Dostrovsky JO. High-frequency synchronization of neuronal activity in the subthalamic nucleus of Parkinsonian patients with limb tremor. J Neurosci 2000;20(20):7766–75.
Medvedev AV. Epileptiform spikes desynchronize and diminish fast (gamma) activity of the brain. An "anti-binding" mechanism? Brain Res Bull 2002;58(1):115–28.
Mormann F, Kreuz T, Andrzejak RG, David P, Lehnertz K, Elger CE. Epileptic seizures are preceded by a decrease in synchronization. Epilepsy Res 2003;53(3):173–85.
Netoff TI, Schiff SJ. Decreased neuronal synchronization during experimental seizures. J Neurosci 2002;22(16):7297–307.
Paxinos G, Watson W. The rat brain in stereotaxic coordinates. New York: Academic Press; 2006.
Roelfsema PR, Engel AK, Konig P, Singer W. Visuomotor integration is associated with zero time-lag synchronization among cortical areas. Nature 1997;385(6612):157–61.
Rosenblum MB, Pikovsky AS, Kurths J. Phase synchronization of chaotic oscillators. Phys Rev Lett 1996;76(11):1804–7.
Roux SG, Cenier T, Garcia S, Litaudon P, Buonviso N. A wavelet-based method for local phase extraction from a multi-frequency oscillatory signal. J Neurosci Methods 2007;160(1):135–43.
Salisbury JI, Wimbush M. Using modern time series analysis techniques to predict ENSO events from the SOI time series. Nonlin Processes Geophys 2002;9:341–5.
Schlurmann T. Spectral frequency analysis of nonlinear water waves derived from the Hilbert–Huang transformation. J Offshore Mech Arctic Eng 2002;124(1):22–8.
Sinclair S, Pegram GGS. Empirical mode decomposition and its algorithms. In: IEEE-EURASIP workshop on nonlinear signal and image processing, 8–11 June 2005, Grado, Italy; 2005.
Zhang RR, Ma S, Safek E, Hartzell S. Hilbert-Huang transform analysis of dynamic and earthquake motion recordings. J Eng Mech 2003;129(8):861–75.